0013-7227/01/$03.00/0
Printed in U.S.A.

Endocrinology 142(10):4195–4202

Rat PPARs: Quantitative Analysis in Adult Rat Tissues and Regulation in Fasting and Refeeding

PASCAL ESCHER*, OLIVIER BRAISSANT†, SHARMILA BASU-MODAK‡, LILIANE MICHALIK, WALTER WAHLI, AND BÉATRICE DESVERGNE

Institut de Biologie Animale, Université de Lausanne, CH-1015 Lausanne, Switzerland

PPARs are members of the nuclear hormone receptor superfamily and are primarily involved in lipid metabolism. The expression patterns of all 3 PPAR isotypes in 22 adult rat organs were analyzed by a quantitative ribonuclease protection assay. The data obtained allowed comparison of the expression of each isotype to the others and provided new insight into the less studied PPARβ (NR1C2) expression and function. This isotype shows a ubiquitous expression pattern and is the most abundant of the three PPARs in all analyzed tissues except adipose tissue. Its expression is especially high in the digestive tract, in addition to kidney, heart, diaphragm, and esophagus. After an overnight fast, PPARβ mRNA levels are dramatically down-regulated in liver and kidney by up to 80% and are rapidly restored to control levels upon refeeding. This tight nutritional regulation is independent of the circulating glucocorticoid levels and the presence of PPARα, whose activity is markedly up-regulated in the liver and small intestine during fasting. Finally, PPARγ2 mRNA levels are decreased by 50% during fasting in both white and brown adipose tissue. In conclusion, fasting can strongly influence PPAR expression, but in only a few selected tissues. (*Endocrinology* 142: 4195–4202, 2001)

PPARs ARE LIGAND-ACTIVATED transcription factors belonging to the nuclear hormone receptor superfamily. This superfamily is characterized by a common structural organization in functional domains: the amino-terminal A/B domain mediates ligand-independent *trans*-activation functions; the C domain contains a highly conserved zinc finger structure forming the DNA-binding domain and a dimerization interface; the D domain is a structurally poorly defined hinge region; the carboxyl-terminal E/F domain or ligand-binding domain mediates ligand-dependent *trans*activation and dimerization (1). Three PPAR isotypes, *i.e.* PPARα (NR1C1); PPARβ (NR1C2), which is also called PPARδ, NUC-1, or FAAR; and PPARγ (NR1C3), have been reported in vertebrates as primitive as cyclostoma (2), in lower vertebrates (3), and in mammals (4). In mammals, alternative promoter usage and differential splicing of the *pparγ* gene transcripts yield two isoforms, γ1 and γ2 (5). In human, a PPARγ3 mRNA is transcribed from a third promoter, resulting in a protein identical to PPARγ1 (6).

PPAR heterodimerizes with the 9-*cis* RXR to bind DR1 (direct repeat spaced by 1 bp) response elements, called PPAR response element, identified in the promoters of target genes involved in microsomal ω-hydroxylation, peroxisomal β-oxidation, mitochondrial β-oxidation, ketogenesis, lipoprotein metabolism, fatty acid binding, and fatty acid transport (7). Various ligands have been described for PPARs: natural fatty acids, especially polyunsaturated ones; arachidonate derivatives; hypolipidemic fibrates; and insulin-sensitizing thiazolidinediones (8). The nature of these PPAR ligands together with the function of identified target genes suggest that PPARs play a key role in lipid and glucose metabolism and homeostasis. PPARs are expressed in a broad range of tissues in adult rodents, as previously shown by *in situ* hybridization (9). PPARα is expressed in cells with high catabolic rates of fatty acids and high peroxisomedependent activities (hepatocytes, cardiomyocytes, proximal tubules of kidney, brown adipocytes, and intestinal mucosa) (4, 9). PPARα-null mutant mice allowed identification of this isotype as a mediator of the pleiotropic effects of peroxisome proliferators in liver (10). This isotype is the best studied to date during fasting. Elevated glucocorticoid hormone levels, observed during fasting and stress, up-regulate hepatic PPARα expression at the transcriptional level through binding of GRs to response elements located in the promoter of PPARα (11–15). The critical role of PPARα in lipid catabolism as well as glucose homeostasis is revealed unequivocally during fasting, where PPARα-null mutant mice show abnormally elevated FFA fasting levels. This indicates a dramatic inhibition of hepatic fatty acid oxidation that results in hepatic steatosis, myocardial lipid accumulation, hypoketonemia, hypoglycemia, and hypothermia (16, 17). PPARβ is expressed ubiquitously and is abundant in most tissues (4, 9, 18). PPARβ (also often called PPARδ) function has been recently linked to basal lipid metabolism, embryo implantation, colon cancer, and inflammation (19–22). PPARγ expression is restricted mainly to adipose tissue and large intestine, with some expression in parts of the immune system (4, 9). Several loss of function experiments in mice have shown that PPARγ is important in placental development and is required for adipogenesis *in vivo* (23–25).

Previous *in situ* hybridization studies in adult rat have demonstrated that PPARs are expressed in specific cell populations or restricted areas of a given tissue (9). However, information concerning the relative expression level of each PPAR isotype with respect to the two others is presently lacking. We thus quantitatively studied PPAR mRNA ex-

Abbreviations: BAT, Brown adipose tissue; NFDM TBS-Tween, 5% nonfat dry milk in 25 mM Tris-HCl (pH 8.0), 140 mM NaCl, 2 mM KCl, and 0.05% Tween 20; nt, nucleotides; RNase, ribonuclease; WAT, white adipose tissue.

pression for each of the three PPAR isotypes by ribonuclease (RNase) protection assay in 22 different organs of the adult rat in the fed state, during an overnight fast, and after refeeding. This provides valuable physiological information about the particular and sometimes opposite effects for which the three PPAR isotypes are responsible.

Materials and Methods

Cloning of the rat PPARs

The full-length cDNAs of rat PPARs were obtained by RT-PCR, using the Expand Reverse Kit (Roche Molecular Biochemicals, Indianapolis, IN). Total rat liver RNA was used for cloning rat (r)PPARα and rPPARβ and total white adipose tissue (WAT) RNA for cloning rPPARγ1 and rPPARγ2, with the following downstream primers in the reverse transcriptase reaction: 5′-ATCTCAGGATCCATCAGTACATGTCTCTGT-3′ (rPPARα), 5′-CTGCGTGGATCCTTAGTACATGTCCTTGTA-3′ (rPPARβ), and 5′-GGTGGGGAATTCCTGCTAATACAAGTCCTT-3′ (rPPARγ).

The following upstream primers were added for subsequent PCR amplification: 5′-CCACAAGGATCCAACATGGTGGACACAGAG-3′ (rPPARα), 5′-CAAGTGGGATCCGTCATGGAACAGCCACAG-3′ (rPPARβ), 5′-TTACTGGAATTCCCATGGTTGACACAGAGA-3′ (rPPARγ1), and 5′-TCTGTTGAATTCTGTTATGGGTGAAACTCT-3′ (rPPARγ2).

The PCR products were subcloned by using the Rapid DNA Ligation Kit (Roche Molecular Biochemicals) into pCRII vector (Invitrogen, San Diego, CA) resulting in pCR-rPPARα, pCR-rPPARβ, pCR-rPPARγ1, and pCR-rPPARγ2 recombinant vectors. Two independent clones of each isotype and isoform were sequenced manually on both strands using the T7 Polymerase Sequencing Kit with [α-^{35}S]deoxy-CTP [Amersham Pharmacia Biotech (Arlington Heights, IL) and Hartmann Analytik (Braunschweig, Germany)].

Probes for RNase protection assay

A *Bam*HI/*Eco*RI fragment was excised from a partial L27 (large ribosomal subunit, 27-kDa protein) cDNA [155–374 nucleotides (nt)] (11) and subcloned into the pBluescript KS$^-$ vector (Stratagene, La Jolla, CA). The resulting construct pBS-L27 (150 nt) was digested by *Eco*RI, transcribed by T7 polymerase (Promega Corp.) yielding a 200-bp riboprobe and a digested fragment of 150 bp. We used a previously described 287-bp probe located in the E/F domain to assess rPPARα mRNA expression (11). The plasmid pCR-rPPARβ was digested by *Xba*I and *Bgl*II and the 171-bp fragment containing the 3′-end of the E/F domain subcloned into the pBluescript SK$^+$ vector (Stratagene) digested by *Xba*I and *Bam*HI to obtain the recombinant plasmid pBS-rPPARβ (171 nt). A 215-bp antisense probe was synthesized by T7 RNA polymerase (Promega Corp., Madison, WI) transcription of pBS-rPPARβ (171 nt) linearized by *Xba*I, resulting in a protected fragment of 171 bp for rPPARβ. The plasmid pCR-rPPARγ2 was digested by *Pvu*II and *Eco*RI, and the 351-bp fragment containing the 5′ of the A/B domain was subcloned into the pBluescript KS$^+$ vector (Stratagene) digested by *Sma*I and *Eco*RI to obtain the recombinant plasmid pBS-rPPARγ (351 nt). A 409-bp antisense riboprobe was synthesized by T7 RNA polymerase (Promega Corp.) transcription of this plasmid linearized by *Hin*dIII, resulting in a protected fragment of 351 bp for rPPARγ2 and 257 bp for rPPARγ1. The G+C content of the probes is 51.2% for rPPARα, 60.2% for rPPARβ, 51.4% for rPPARγ1, and 50.4% for rPPARγ2, with calculated T_m of 73.0, 71.7, 72.8, and 73.4 C, respectively.

To assess mRNA expression of mouse PPARs, we constructed the following probes. A *Bam*HI/*Kpn*I fragment (nt 160–503 of GenBank accession no. X57638) encoding the A/B domain was excised off a pSG5-mouse (m)PPARα vector and subcloned into the *Bam*HI/*Kpn*I sites of pBluescript SK$^+$ (Stratagene). The recombinant plasmid pBSmPPARα (333 nt) was linearized by *Xba*I, and a 369-bp antisense riboprobe was transcribed by T7 RNA polymerase (Promega Corp.), yielding a protected fragment of 333 bp. A pSG5-mPPARβ vector was digested by *Sma*I/*Xho*I, and a fragment coding for partial A/B and C domains (nt 31–315 of GenBank accession no. U10375) was subcloned into pBluescript KS$^+$ (Stratagene). The recombinant plasmid pBSmPPARβ (288 nt) was linearized by *Xba*I, and a 328-bp antisense riboprobe was transcribed by T3 RNA polymerase (Promega Corp.), resulting in a protected fragment of 288 bp. A fragment spanning nt 910-1093 of GenBank accession no. U01841 and encoding the partial D and E/F domain of mPPARγ was cut off of a pCMV-mPPARγ vector and subcloned into the *Hin*dIII/*Sma*I sites of pBluescript KS$^+$ vector (Stratagene). An antisense riboprobe of 237 bp was transcribed by T7 RNA polymerase (Promega Corp.) from the recombinant plasmid pBSmPPARγ (185 nt) linearized by *Hin*dIII, yielding a protected fragment of 185 bp. To assess mouse L27 mRNA expression we used the rat pBS-L27 (150 nt) probe described above.

For all PPAR probes, a 1:1 ratio of [α-^{32}P]UTP (800 Ci/mmol) to cold UTP was used, whereas a 1:20 ratio was used for the L27 probe. Labeled probes were precipitated by trichloroacetic acid on GM filters (Whatman, Clifton, NJ) to determine radioisotope incorporation, which was typically between 60–70%. Filters were counted using an automatic liquid scintillation system (Kontron Instruments Ltd., Zurich, Switzerland), and specific activities were calculated. In pilot experiments, each probe was hybridized with increasing amounts of sample RNA (5–40 μg), ensuring that 1 ng specific PPAR probes and 10 ng L27 probe provided a molar excess of probe *vs.* target RNA up to the maximal amount of RNA tested.

RNA preparation and RNase protection assay

Eight- to 9-wk-old male Sprague Dawley (~200 g) rats were purchased from RCC BRL (Basel, Switzerland). Eight- to 12-wk-old male pure-bred wild-type or PPARα null mice on an Sv129 background were obtained from Dr. Frank Gonzalez (10). Rats and mice were housed with a 12-h light, 12-h dark cycle beginning at 0700 h and free access to water and standard laboratory chow. For the fasting experiment, food was removed at 1900 h. Access to water remained free, and animals were killed the following day at 0700 h. In the refeeding experiment, food was reintroduced after 7.5 h of fasting. Dexamethasone was injected into rats at 40 μg/kg BW, and rats were killed 4 h later. Animals were anesthetized with Forene (Abbott Laboratories, Chicago, IL), killed by decapitation, and rapidly dissected. Tissues were directly frozen in TRIzol (Life Technologies, Inc., Grand Island, NY) by liquid nitrogen and kept at −70 C until RNA preparation. Tissues were homogenized with a Polytron homogenizer (Kinematica, Lucerne, Switzerland), and total RNA was prepared with TRIzol following the instructions of the provider. The RNase protection assay was carried out as previously described (11). Approximately 15 μg total RNA were hybridized to 1 ng specific PPAR probes each (2×10^9 cpm/μg) and 10 ng L27 probe (1×10^8 cpm/μg). RNase digestion [RNase A, Sigma (St. Louis, MO); RNase T1, Life Technologies, Inc.] was carried out for all the probes at 30 C. Gels were exposed on phosphor screens of a StormImager 840 (Molecular Dynamics, Inc., Sunnyvale, CA). IQuant 2.5 software (Molecular Dynamics, Inc.) was used for quantification by drawing a line per lane and removing background. PPAR mRNA expression was normalized to the previously calculated specific activity of the probe and to L27 mRNA expression. The PPAR/L27 ratio was further normalized to the UTP content of each PPAR probe. SD values were calculated with Excel software (Microsoft Corp., Redmond, VA) and Cricket Graph software (Computer Associates, Islandia, NY) used for diagrams.

All animal experimentation was approved by the commission of the Etat de Vaud (Switzerland) for authorization of live animal experimentation.

Western blot analysis

Nuclear extracts of rat liver were prepared as follows. One gram of rat liver was frozen in liquid nitrogen and crushed with a hammer. Tissues were further homogenized in 5 ml of a 0.5 M sucrose, 50 mM Tris-HCl (pH 7.5), 1 mM EDTA, and 25 mM KCl solution in a glass-Teflon homogenizer. Cells were then lysed with 0.5% Triton X-100 for 30 min at 4 C. The homogenate was layered on a 0.9 M sucrose, 50 mM Tris-HCl (pH 7.5), 1 mM EDTA, and 25 mM KCl solution. After centrifugation at $1800 \times g$ for 20 min, pelleted nuclei were resuspended in 40% glycerol, 50 mM Tris-HCl (pH 8), 5 mM $MgCl_2$, and 0.1 mM EDTA and stored at −70 C. The protein concentration was determined by measuring absorbance at 230 and 260 nm. Thirty-five micrograms of proteins were separated by SDS-PAGE and blotted on a BA85 Protrane membrane (Schleicher & Schuell, Inc., Keene, NH). PPARβ antibody was raised

against the first 15 N-terminal amino acids of mPPARβ (peptide sequence: MEQPQEETPEAREEEC). Blots were blocked for 1 h at 37 C with 5% nonfat dry milk in 25 mM Tris-HCl (pH 8.0), 140 mM NaCl, 2 mM KCl, and 0.05% Tween 20 (NFDM TBS-Tween) and washed twice for 10 min each time in TBS-Tween. Primary antibody was incubated for 4 h at a final concentration of approximately 2 μg/ml in 0.5% NFDM TBS-Tween, and blots were washed twice for 10 min each time in 0.5% NFDM TBS-Tween. A secondary goat antirabbit IgG peroxidase-conjugated antibody was incubated for 1 h at a dilution of 1:3000 in 0.5% NFDM TBS-Tween, and blots were washed twice for 10 min each time in 0.5% NFDM TBS-Tween and twice for 30 min each time in 5% NFDM TBS-Tween. Immunodetection and chemiluminescence were performed according to the manufacturer's protocol (ECL, Amersham Pharmacia Biotech), and membranes were exposed on Kodak films. Signals were quantified using an Elscript 400-AT/SM densitometer (Hirschmann, Neuried, Germany).

Results

Cloning and sequencing of rat PPAR cDNAs

First, we cloned and sequenced all three rat PPAR isotype cDNAs, including that of the PPARγ2 isoform, to have access to adequate probes for further mRNA expression studies. The sequence of rPPARα is identical to that reported previously (26). For rPPARβ we found an A at position 1028, yielding Asp^{343} as in all known other mammal PPARs, instead of the previously reported T yielding Val^{343} (18). In the rPPARγ2 sequence we read CG at positions 330 and 331 yielding Arg^{111} instead of GC yielding the reported Ala^{111} (27, 28). As our sequence is based on two independent RT-PCR reactions for both rPPARγ1 and rPPARγ2, a polymorphism at this site in exon 2 of the *pparγ* gene may therefore exist.

PPAR expression in rat tissues

PPAR mRNA expression for each of the three PPAR isotypes was quantified by RNase protection assay in 22 different organs of the adult rat. All experiments were performed so as to allow a comparison of the relative levels between the different tissues and between the different isotypes (see *Materials and Methods*).

In nearly all tissues analyzed, PPARβ is the most abundant isotype, with its highest expression levels in the digestive tract, kidney, heart, diaphragm, and esophagus (Figs. 1 and 2B). In comparison to the highest levels in the digestive tract, PPARβ expression is about 4–5 times lower in all of the other organs analyzed. PPARα is highly expressed in brown adipose tissue (BAT), at about 4 times the levels observed in liver, heart, diaphragm, esophagus, and kidney (Figs. 1 and 2A). It is indeed the highest PPAR level regardless of the isotype or tissue considered (Fig. 2). With respect to its expression in liver, PPARα is expressed at about 3-fold lower levels in small intestine, bladder (data not shown), and skeletal muscle. In all other tissues, including WAT, PPARα mRNA remains detectable, but at low levels. In the digestive tract, PPARα mRNA expression decreases from the duodenum and ileum toward the rectum. PPARγ1 is highly expressed in both WAT and BAT at levels comparable to those of PPARα mRNA in BAT and PPARβ mRNA in the digestive tract (Figs. 1 and 2C). PPARγ1 is expressed in colon and cecum at about 3-fold lower levels than in adipose tissue. PPARγ1 expression in spleen, stomach, rectum, lung, and heart is about 10 times lower than that in adipose tissue and at least 25 times lower in small intestine, testis, kidney, and liver. The presence of both PPARγ isoforms has been consistently found in lung, WAT, BAT, and skeletal muscle, and the relative amount of PPARγ2 mRNA *vs.* total PPARγ mRNA is, respectively, 33%, 30%, 18%, and 32% (Figs. 1 and 2D).

We also analyzed rat tissues of three female rats and compared the PPAR mRNA levels between male and female animals (data not shown). No tissue showed a gender-specific PPAR mRNA expression pattern.

PPAR mRNA expression during fasting

We compared the mRNA expression of all three PPAR isotypes in overnight-fasted male adult rats with that of their fed counterparts. In an attempt to synchronize the feeding status, food was removed at the end of the daylight hours, when rats do not feed extensively. The rats were killed after a 12-h fast at the end of the dark cycle.

Strikingly, we observed a dramatic decrease in PPARβ mRNA in the liver and kidney by, respectively, 75% and 80% (Fig. 2B). In none of the other analyzed tissues did we observe any statistically significant variations in PPARβ mRNA levels (Fig. 2B). PPARα mRNA levels increase in the liver during fasting as previously reported (13) (Fig. 2A). We also observed a statistically significant increase in PPARα expression in duodenum, jejunum, and colon by 40%, 57%, and 20%, respectively, and a marked increase in the ileum by 38%. A significant increase in PPARα expression was also found in the thymus, where absolute PPARα expression is very low (Fig. 2A). Interestingly, PPARγ2 mRNA levels decreased in WAT and BAT by up to 50% during fasting (Fig. 2D), whereas PPARγ1 showed only a weak regulation during fasting, with a decreased mRNA expression level that was only significant in the ileum (Fig. 2C).

Nutritional regulation of PPARβ mRNA expression in liver and kidney

We then performed a refeeding experiment to study the potential regulation of hepatic and renal PPARβ mRNA expression by food intake. The experiment started at the end of the daylight hours. The group of refed rats was first fasted for 7.5 h and then had free access to food for 4.5 h before mRNA levels were measured. Control groups in this experiment comprised fed rats and rats fasted for 7.5 and 12 h (7.5 plus 4.5 h), respectively. We assessed PPARα and PPARβ mRNA expression by RNase protection assay in liver, kidney, heart, and WAT (Fig. 3A). Again, we observed in both liver and kidney a dramatic decrease in PPARβ mRNA expression after both 7.5 and 12 h of fasting by up to 70% ($P < 0.05$; Fig. 3B). Refeeding for 4.5 h after a 7.5-h fast was sufficient to restore PPARβ mRNA expression to the level observed in fed animals (Fig. 3B). Concomitant to the decrease in mRNA levels, PPARβ protein abundance also decreased by about 30% during fasting, as assessed by a semiquantitative Western blot on liver nuclear extracts (Fig. 4).

As a positive control of PPAR mRNA regulation during fasting, we assessed PPARα mRNA expression in liver, kidney, and heart (Fig. 3A). We again observed a significant more than 2.5-fold increase in PPARα mRNA gene expres-

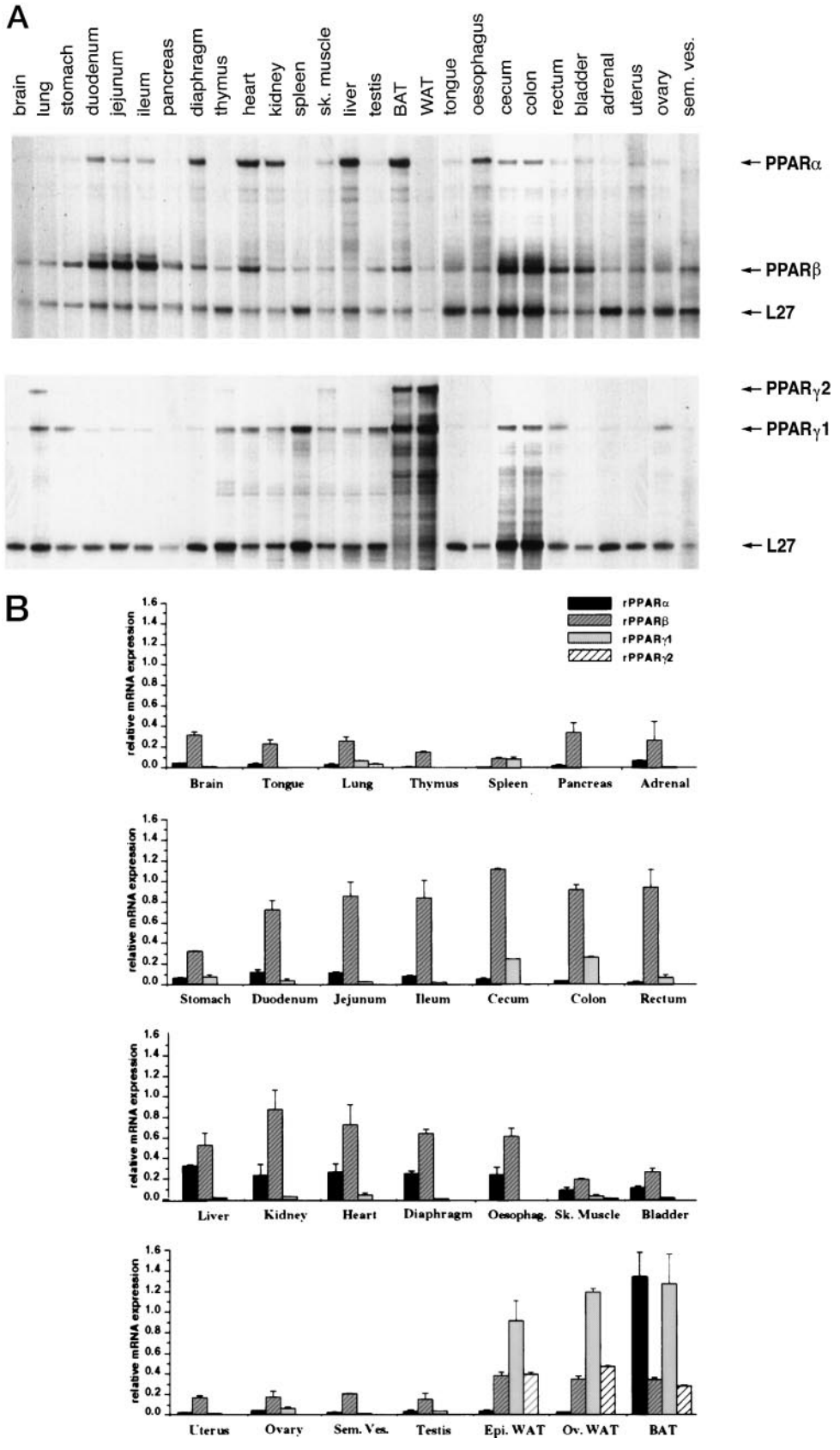

FIG. 1. Comparative analysis of PPARα, PPARβ, and PPARγ expression in 22 organs. A, RNase protection assay. rPPARα and rPPARβ mRNA expression (*top panel*) and rPPARγ mRNA expression (*bottom panel*) detected by RNase protection assay using total rat RNA samples from different organs. Fifteen micrograms of total RNA were used per RNase protection assay, and the samples were separated on a 6% polyacrylamide

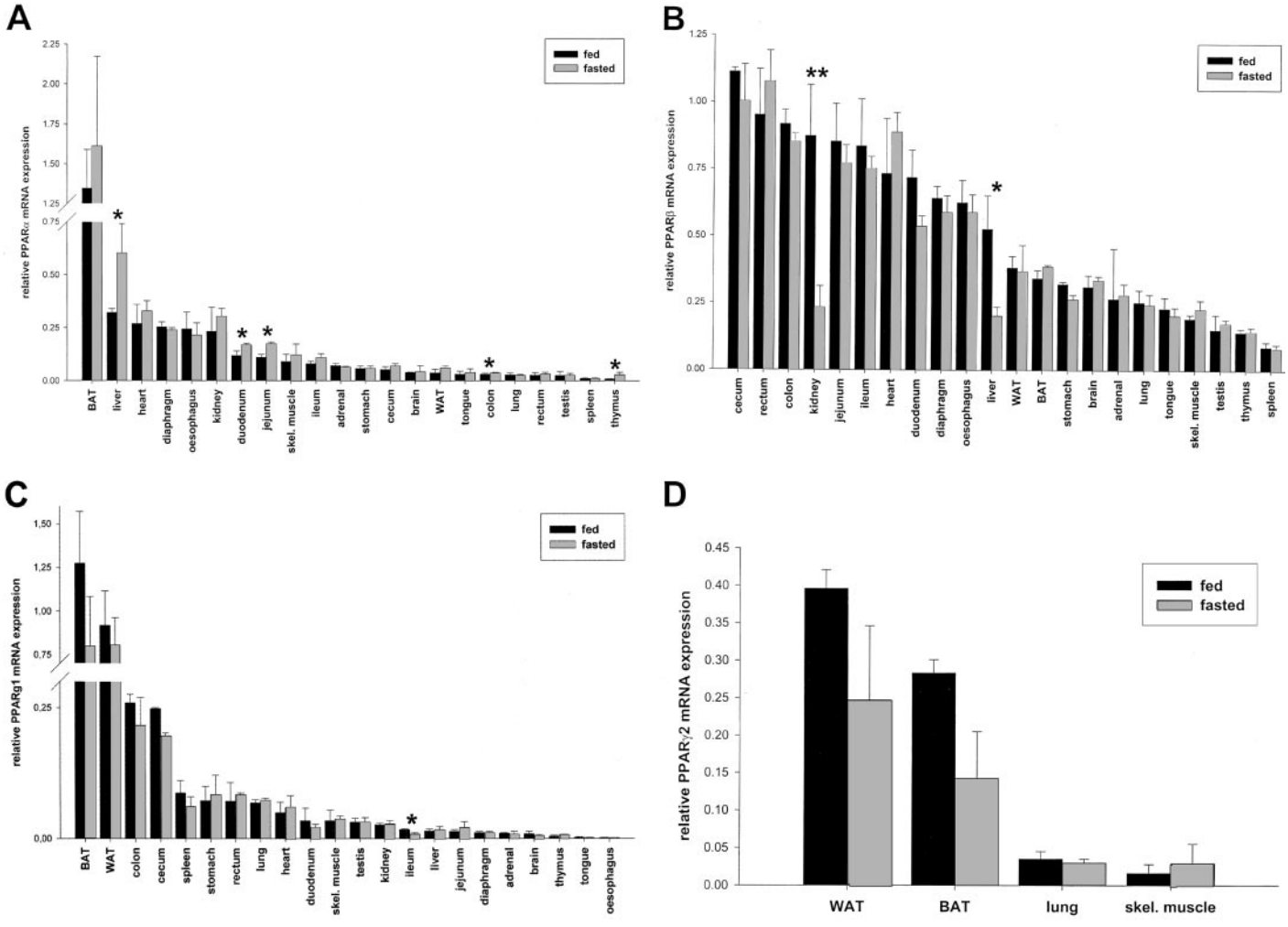

FIG. 2. PPAR mRNA expression during fasting in adult rat tissues. Fifteen micrograms of total RNA from fed and overnight-fasted adult rat tissues were analyzed for PPAR mRNA expression by RNase protection assay. After RNase digestion, the samples were separated on a 6% polyacrylamide gel, as illustrated in Fig. 1. Histograms show quantifications (in relative values) of PPAR mRNA levels ± SD, normalized to L27 mRNA expression, derived from RNase protection assays such as that illustrated in Fig. 3. Relative PPAR mRNA expression levels are drawn so as to allow comparison between different isotypes and organs (see *Materials and Methods*). A, PPARα mRNA expression; B, PPARβ mRNA expression; C, PPARγ1 mRNA expression; D, PPARγ2 mRNA expression. n = 5 for liver, heart, kidney, brain, and WAT; n = 3 for all other tissues. skel. Muscle, Skeletal muscle. *, $P < 0.05$; **, $P < 0.01$ (by *t* test).

sion during fasting in the liver ($P < 0.05$; Fig. 3C). Renal and cardiac PPARα mRNA expression levels were not increased in a significant manner ($P > 0.05$; Fig. 3C).

Nutritional hepatic regulation of PPARβ is independent of PPARα

To further understand the opposite regulation of PPARα and PPARβ mRNA expression in liver during fasting, we used PPARα-null mutant mice to investigate whether the observed tight nutritional regulation of hepatic PPARβ gene expression is dependent on PPARα activity. The design of specific mouse PPAR probes allowed us to assess PPARβ mRNA expression in wild-type and mutant mice by RNase protection assay (Fig. 5A). After an overnight fast, we observed a similar decrease in hepatic PPARβ mRNA expression in wild-type and PPARα null-mutant mice by up to 80% (Fig. 5B). Thus, nutritional regulation of hepatic PPARβ mRNA expression by fasting is independent of the activity of PPARα. A parallel analysis of PPARγ mRNA expression by RNase protection showed similar expression levels of this latter subtype in both wild-type and mutant mice, thus excluding compensatory effects of the PPARγ isotype in the absence of PPARα (data not shown).

Finally and in contrast to PPARα (13), the regulation of

gel. The protected fragments have a size of 287 nt for rPPARα, 171 nt for rPPARβ, 257 nt for rPPARγ1, and 351 nt for rPPARγ2. Ribosomal protein L27 was used as an internal standard. Representative results of different experiments or different exposure times are presented. PPAR and L27 protected fragments are indicated by *arrows*. B, Histograms show quantifications (in relative values) of PPAR mRNA levels ± SD, normalized to L27 mRNA expression, derived from RNase protection assays such as that illustrated in A. Relative PPAR mRNA expression levels are drawn so as to allow comparison between different isotypes and organs. n = 5 for liver, heart, kidney, brain, and WAT; n = 3 for all other tissues. sem. vesicle, Seminal vesicle; sk. Muscle, skeletal muscle.

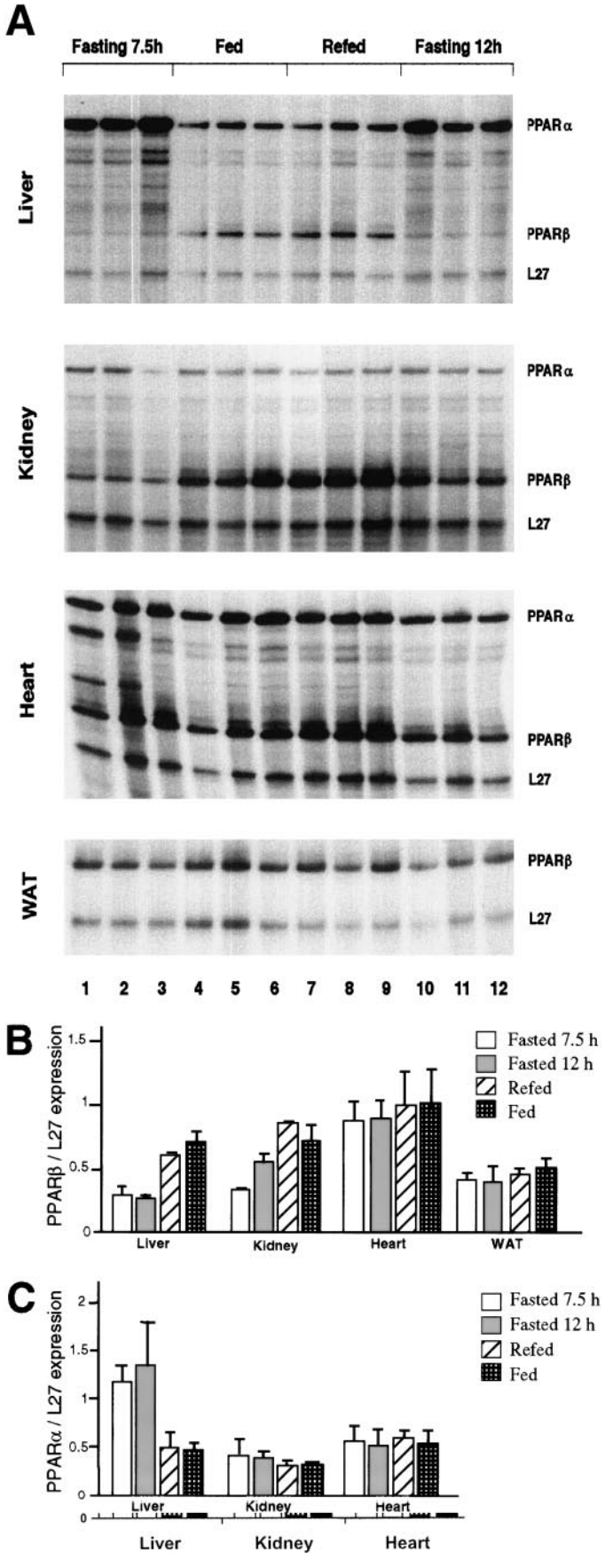

hepatic PPARβ mRNA expression levels by fasting and refeeding is independent of plasma glucocorticoid levels, as injection of the synthetic glucocorticoid dexamethasone had no effect on hepatic PPARβ mRNA expression (data not shown).

Discussion

PPARβ is predominantly expressed in the digestive tract and in organs with high fatty acid oxidation

The present study gives new insight into the physiological function of PPARβ. PPARβ is the most abundant isotype in all adult rat tissues analyzed, except adipose tissue. Previous *in situ* hybridization studies showed that PPARβ is highly expressed in proliferating embryonic tissues (29). High PPARβ expression in the digestive tract may therefore be linked to ongoing cell proliferation and differentiation processes in the adult gut. Indeed, enterocytes have a high turnover of 3–6 d in the small intestine and 5–8 d in the large intestine (30). Interestingly, PPARβ has been identified as a β-catenin/Tcf-4 target gene in humans, like other growth-promoting genes, such as c-*myc* and cyclin D1 (21).

The predominant expression of PPARβ in intestine also suggests a potential role for this isotype in processes linked to food intake and lipid metabolism. The mucosa of the small intestine resorbs diet lipids that enterocytes transport via the cytosolic fatty acid-binding proteins toward the smooth endoplasmic reticulum to resynthesize lipids and triglycerides (30). In stomach, where no resorption of nutrients occurs, PPARβ expression is about 2 times lower than that in intestine. A recent report using the PPARβ-selective ligand GW2433 in PPARα-null mutant mice shows that the high levels of PPARβ present in the small intestine are sufficient to *trans*-activate the *liver fabp* gene, which is a PPARα target gene in the liver (31). PPARβ may therefore regulate the intestinal expression of other PPAR target genes implicated in lipid metabolism for which a PPARα-dependent *trans*-activation has been previously observed in liver.

The potential role of PPARβ in metabolism is further underscored by our observation that tissues with high metabolic rate, such as liver, kidney, and oxidative muscles, also express PPARβ mRNA at high levels. Among muscular tissues, we observe a concomitant decrease in PPARα and PPARβ expression with decreasing importance of fatty acid oxidation, *i.e.* skeletal muscle and bladder show lower expression levels of both PPARα and PPARβ compared to heart and diaphragm. Taken together, these observations suggest

FIG. 3. PPAR mRNA expression in fasting and refeeding. A, Fifteen micrograms of total liver, kidney, heart, and WAT RNA were analyzed by RNase protection assay for PPARα and PPARβ mRNA expression. After RNase digestion, the samples were separated on a 6% polyacrylamide gel. Adult rats were fasted for 7.5 h (lanes 1–3) or 12 h (lanes 10–12), control animals were fed *ad libitum* overnight (lanes 4–6), and refed animals were fasted for 7.5 h, then *ad libitum* feeding was reintroduced for 4.5 h before killing the animals (lanes 7–9). B, Histogram of PPARβ mRNA expression in liver, kidney, heart, and WAT standardized to L27 expression. The mean of three animals ± SD are shown. C, Histogram of PPARα mRNA expression in liver, kidney, and heart standardized to L27 expression. The mean of three animals ± SD are shown.

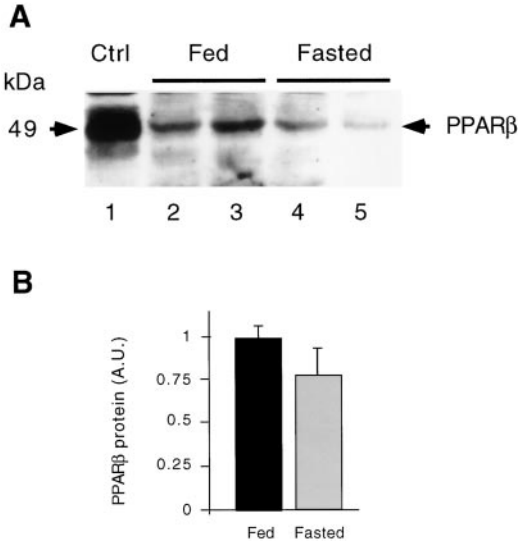

FIG. 4. Western blot analysis of PPARβ expression in liver nuclear extracts of fed and 12-h fasted rats. A, Thirty-five micrograms of hepatic nuclear proteins were loaded on an SDS gel and probed after Western blotting with an antimouse PPARβ antibody. As a positive control we used 20 μg of a total protein extract from COS-1 cells transiently transfected with a pSG5-rat PPARβ expression vector (lane 1). A major band with an expected size of 49 kDa for PPARβ was detected by chemiluminescence in the liver nuclear extracts of fed (lanes 2 and 3) and fasted (lanes 4 and 5) rats. B, Histogram of PPARβ protein expression in fed and fasted animals (n = 4). Signals were quantified with a densitometer and are reported in arbitrary units (A.U.). The mean of four animals ± SD are shown.

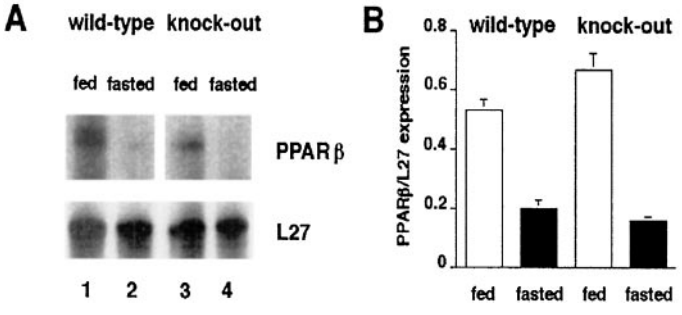

FIG. 5. Fasting in PPARα-null mutant mice. Wild-type and mutant mice were fasted overnight. A, PPARβ mRNA expression was analyzed by RNase protection assay on 5 μg total liver RNA. After RNase digestion, the samples were separated on a 6% polyacrylamide gel. B, Histogram of PPARβ mRNA expression standardized to L27 mRNA expression (n = 2).

that in tissues where fatty acid oxidation is used for energy production, a link between PPARβ and the necessary high lipid metabolism may exist.

Fasting specifically up-regulates hepatic and intestinal PPARα expression

Among all tissues analyzed, only the liver and small intestine show increased PPARα mRNA expression during fasting. The high fasting PPARα mRNA levels observed in the liver underline the prominent role of this isotype in hepatic lipid metabolism. Up-regulation of hepatic PPARα expression and subsequent activation of the PPARα target genes implicated in hepatic fatty acid oxidation (*i.e.* mitochondrial β-oxidation, microsomal ω-hydroxylation, and peroxisomal β-oxidation) are critical events in the adaptive response to fasting (16, 17, 32). In addition to the liver, PPARα induces cardiac fatty acid oxidation during fasting (17). Interestingly, we observed no increase in PPARα mRNA expression during fasting in this oxidative muscle. In kidney also, PPARα mRNA expression is not markedly increased, although fatty acids are efficiently oxidized in the renal cortex. These results are in line with the observation that clofibrate-fed rats show an increase in cortical expression of mitochondrial and peroxisomal PPARα target genes, whereas no significant change in PPARα mRNA itself is observed (33).

Interestingly, GR mRNA levels are comparable in liver, kidney, and heart (34), but corticosteroids do not modulate its expression in the two latter tissues (35). Additional experiments will be necessary to determine whether the GRs present in the intestinal epithelium (36) mediate the observed increase in intestinal PPARα mRNA expression.

Nutritional regulation of PPARβ mRNA expression

An important finding of this study is the dramatic decrease in hepatic and renal PPARβ mRNA expression during fasting, which is rapidly restored to control levels by refeeding. In agreement with a regulation of PPARβ by food intake and in addition to our results, a recent report shows that PPARβ mRNA expression levels remain low after a 72-h fast (37). We observe a general tendency toward decreased PPARβ mRNA levels during fasting in all analyzed tissues, but the tight regulation by feeding status in liver and kidney suggests a tissue-specific mechanism of PPARβ regulation. Our results show that PPARβ regulation during fasting is independent of plasma glucocorticoid hormone levels and PPARα activity. Also, the abnormally elevated plasma FFA concentrations observed in the PPARα-null mutant mice (16) do not alter the expression of PPARβ compared with that in wild-type mice. Thus, serum lipid levels alone are not sufficient for the nutritional regulation of PPARβ. The observation that PPARβ is down-regulated in both the liver and kidney, but PPARα is up-regulated only in the liver, further suggests different regulatory mechanisms involved in the expression of these two PPAR isotypes during fasting.

The similar regulation of PPARβ expression in the liver and kidney may be related to metabolic fates common to these two tissues, *e.g.* gluconeogenesis and lipogenesis. As gluconeogenesis is increased during fasting, PPARβ would be a negative regulator of this pathway. Interestingly, sterol regulatory element-binding protein-1c/adipocyte determination differentiation-dependent factor-1 shows a similar expression pattern as PPARβ during fasting and refeeding (38, 39). This transcription factor is induced by food intake and mediates the expression of lipogenic genes induced by glucose and insulin (40). Further studies will be necessary to determine whether PPARβ is implicated in sensing serum carbohydrate levels and is targeted by hormonal signaling leading to lipogenesis.

Acknowledgments

We thank Thomas Lemberger for providing dexamethasone-treated rat RNA samples; Sander Kersten for providing the mouse RNA sam-

ples; Frank Gonzalez for providing PPARα null mutant mice; Daniel Bachmann, Mai Perroud, and Nathalie Deriaz for expert technical help; and Michael Man for excellent advice in statistical analysis. pSG5-mPPARα was a kind gift of S. Green, pSG5-mPPARβ of P. Grimaldi and pCMV-mPPARγ of R. Evans.

Received February 26, 2001. Accepted July 6, 2001.

Address all correspondence and requests for reprints to: Dr. Beatrice Desvergne or Dr. Walter Wahli, Institut de Biologie Animale, Université de Lausanne, CH-1015 Lausanne, Switzerland. E-mail: beatrice.desvergne@iba.unil.ch or walter.wahli@iba.unil.ch.

This work was supported by the Etat de Vaud and grants from the Swiss National Science Foundation (to B.D. and W.W.) and Marie Heim-Vögtlin Fellowship 3234-44994 (to S.B.-M.) of the Swiss National Science Foundation. The nucleotide sequences reported in this paper have been submitted to the EMBL Nucleotide Sequence Database with accession number Y12882 for rat PPARγ2 and AJ306400 for rat PPARβ.

* Present address: Pfizer Global Research and Development, Ann Arbor Laboratories, Molecular Sciences, 2800 Plymouth Road, Ann Arbor, Michigan 48105.

† Present address: Laboratoire de Chimie Clinique, Center Hospitalier Universitaire Vaudois, 1011 Lausanne, Switzerland.

‡ Present address: Department of Pharmacy and Pharmacology, University of Bath, Claverton Down, Bath, United Kingdom BA2 7AY.

References

1. **Mangelsdorf DJ, Thummel C, Beato M, et al.** 1995 The nuclear receptor superfamily: the second decade. Cell 83:835–839
2. **Escriva H, Safi R, Hanni C, et al.** 1997 Ligand binding was acquired during evolution of nuclear receptors. Proc Natl Acad Sci USA 94:6803–6808
3. **Dreyer C, Krey G, Keller H, Givel F, Helftenbein G, Wahli W** 1992 Control of the peroxisomal β-oxidation pathway by a novel family of nuclear hormone receptors. Cell 68:879–887
4. **Kliewer SA, Forman BM, Blumberg B, et al.** 1994 Differential expression and activation of a family of murine peroxisome proliferator-activated receptors. Proc Natl Acad Sci USA 91:7355–7359
5. **Zhu Y, Qi C, Korenberg JR, et al.** 1995 Structural organization of mouse peroxisome proliferator-activated receptor γ (mPPARγ) gene: alternative promoter use and different splicing yield two mPPARγ isoforms. Proc Natl Acad Sci USA 92:7921–7925
6. **Fajas L, Fruchart JC, Auwerx J** 1998 PPARγ3 mRNA: a distinct PPARγ mRNA subtype transcribed from an independent promoter. FEBS Lett 438:55–60
7. **Desvergne B, Wahli W** 1999 Peroxisome proliferator-activated receptors: nuclear control of metabolism. Endocr Rev 20:649–688
8. **Willson TM, Wahli W** 1997 Peroxisome proliferator-activated receptor agonists. Curr Opin Chem Biol 1:235–241
9. **Braissant O, Foufelle F, Scotto C, Dauça M, Wahli W** 1996 Differential expression of peroxisome proliferator-activated receptors (PPARs): tissue distribution of PPAR-α, -β, and -γ in the adult rat. Endocrinology 137:354–366
10. **Lee SS, Pineau T, Drago J, et al.** 1995 Targeted disruption of the alpha isoform of the peroxisome proliferator-activated receptor gene in mice results in abolishment of the pleiotropic effects of peroxisome proliferators. Mol Cell Biol 15:3012–3022
11. **Lemberger T, Staels B, Saladin R, Desvergne B, Auwerx J, Wahli W** 1994 Regulation of the peroxisome proliferator-activated receptor α gene by glucocorticoids. J Biol Chem 269:24527–24530
12. **Steineger HH, Sorensen HN, Tugwood JD, Skrede S, Spydevold O, Gautvik KM** 1994 Dexamethasone and insulin demonstrate marked and opposite regulation of the steady-state mRNA level of the peroxisomal proliferator-activator receptor (PPAR) in hepatic cells. Hormonal modulation of fatty-acid-induced transcription. Eur J Biochem 225:967–974
13. **Lemberger T, Braissant O, Juge-Aubry C, et al.** 1996 PPAR Tissue distribution and interactions with other hormone-signaling pathways. Ann NY Acad Sci 804:231–251
14. **Lemberger T, Saladin R, Vazquez M, et al.** 1996 Expression of the peroxisome proliferator-activated receptor α gene is stimulated by stress and follows a diurnal rhythm. J Biol Chem 271:1764–1769
15. **Sörensen HN, Steineger HH, Eskild W, et al.** Single and clustered glucocorticoid response elements in PPARα 5′-flanking region important for rigid glucocorticoid control of PPARα expression [Abstract 157]. Keystone Symp. 1998
16. **Kersten S, Seydoux J, Peters JM, Gonzalez FJ, Desvergne B, Wahli W** 1999 Peroxisome proliferator-activated receptor α mediates the adaptive response to fasting. J Clin Invest 103:1489–1498
17. **Leone TC, Weinheimer CJ, Kelly DP** 1999 A critical role for the peroxisome proliferator-activated receptor α (PPARα) in the cellular fasting response: the PPARα-null mouse as a model of fatty acid oxidation disorders. Proc Natl Acad Sci USA 96:7473–7478
18. **Xing G, Zhang L, Heynen T, et al.** 1995 Rat PPAR δ contains a CGG triplet repeat and is prominently expressed in the thalamic nuclei. Biochem Biophys Res Commun 217:1015–1025
19. **Basu-Modak S, Braissant O, Escher P, Desvergne B, Honegger P, Wahli W** 1999 Peroxisome proliferator-activated receptor β regulates acyl-CoA synthetase 2 in reaggregated rat brain cell cultures. J Biol Chem 274:35881–35888
20. **Lim H, Gupta RA, Ma W, et al.** 1999 Cyclo-oxygenase-2-derived prostacyclin mediates embryo implantation in the mouse via PPARδ. Genes Dev 13:1561–1574
21. **He T-C, Chan TA, Vogelstein B, Kinzler KW** 1999 PPARδ is an APC-regulated target of nonsteroidal anti-inflammatory drugs. Cell 99:335–345
22. **Peters JM, Lee SST, Li W, et al.** 2000 Growth, adipose, brain, and skin alterations resulting from targeted disruption of the mouse peroxisome proliferator-activated receptor β(δ). Mol Cell Biol 20:5119–5128
23. **Barak Y, Nelson MC, Ong ES, et al.** 1999 PPARγ is required for placental, cardiac, and adipose tissue development. Mol Cell 4:585–595
24. **Kubota N, Terauchi Y, Miki H, et al.** 1999 PPARγ mediates high-fat diet-induced adipocyte hypertrophy and insulin resistance. Mol Cell 4:597–609
25. **Rosen ED, Sarraf P, Troy AE, et al.** 1999 PPARγ is required for the differentiation of adipose tissue in vivo and in vitro. Mol Cell 4:611–617
26. **Göttlicher M, Widmark E, Li Q, Gustafsson JÅ** 1992 Fatty acids activate a chimera of the clofibric acid-activated receptor and the glucocorticoid receptor. Proc Natl Acad Sci USA 89:4653–4657
27. **Tanaka T, Itoh H, Doi K, et al.** 1999 Down regulation of peroxisome proliferator-activated receptorγ expression by inflammatory cytokines and its reversal by thiazolidinediones. Diabetologia 42:702–710
28. **Guardiola-Diaz HM, Rehnmark S, Usuda N, et al.** 1999 Rat peroxisome proliferator-activated receptors and brown adipose tissue function during cold acclimatization. J Biol Chem 274:23368–23377
29. **Braissant O, Wahli W** 1998 Differential expression of peroxisome proliferator-activated receptor-α, -β, and -γ during rat embryonic development. Endocrinology 139:2748–2754
30. **Schmidt RF** 1983 Human physiology. Berlin, Heidelberg, New York: Springer-Verlag
31. **Poirier H, Niot I, Monnot M-C, et al.** 2001 Differential involvement of peroxisome-proliferator-activated receptors α and δ in fibrate and fatty acid-mediated inductions of the gene encoding liver-fatty acid-binding protein in the liver and the small intestine. Biochem J 355:481–488
32. **Kroetz DL, Yook P, Costet P, Bianchi P, Pineau T** 1998 Peroxisome proliferator-activated receptor α controls the hepatic CYP4A induction adaptive response to starvation and diabetes. J Biol Chem 273:31581–31589
33. **Ouali F, Djouadi F, Merlet-Benichou C, Bastin J** 1998 Dietary lipids regulate β-oxidation enzyme gene expression in the developing rat kidney. Am J Physiol 275:F777–F784
34. **Kalinyak JE, Dorin RI, Hoffman AR, Perlman AJ** 1987 Tissue-specific regulation of glucocorticoid receptor mRNA by dexamethasone. J Biol Chem 262:10441–10444
35. **Escoubet B, Coureau C, Blot-Chabaud M, Bonvalet JP, Farman N** 1996 Corticosteroid receptor mRNA expression is unaffected by corticosteroids in rat kidney, heart, and colon. Am J Physiol 270:C1343–C1353
36. **Lentze MJ, Colony PC, Trier JS** 1985 Glucocorticoid receptors in isolated intestinal epithelial cells in rats. Am J Physiol 249:G58–G65
37. **Hashimoto T, Cook WS, Qi C, Yeldandi AV, Reddy JK, Rao MS** 2000 Defect in peroxisome proliferator-activated receptor α-inducible fatty acid oxidation determines the severity of hepatic steatosis in response to fasting. J Biol Chem 275:28918–28928
38. **Horton JD, Bashmakov Y, Shimomura I, Shimano H** 1998 Regulation of sterol regulatory element binding proteis in livers of fasted and refed mice. Proc Natl Acad Sci USA 95:5987–5992
39. **Kim JB, Sarraf P, Wright M, et al.** 1998 Nutritional and insulin regulation of fatty acid synthetase and leptin gene expression through ADD1/SREBP1. J Clin Invest 101:1–9
40. **Foretz M, Pacot C, Dugail I, et al.** 1999 ADD1/SREBP-1c is required in the activation of hepatic lipogenic gene expression by glucose. Mol Cell Biol 19:3760–3768